International Journal of Biological Macromolecules 216 (2022) 291–302

Contents lists available at ScienceDirect

International Journal of Biological Macromolecules

journal homepage: www.elsevier.com/locate/ijbiomac

Photocrosslinkable and self-healable hydrogels of chitosan and hyaluronic acid

Sheila Maiz-Fernández [a,b], Leyre Pérez-Álvarez [a,b,*], Unai Silván [a,c], José Luis Vilas-Vilela [a,b], Senentxu Lanceros-Mendez [a,c]

[a] BCMaterials, Basque Center for Materials, Applications and Nanostructures, UPV/EHU Science Park, 48940 Leioa, Spain
[b] Macromolecular Chemistry Group (LABQUIMAC), Department of Physical Chemistry, Faculty of Science and Technology, University of the Basque Country, UPV/EHU, Barrio Sarriena, s/n, 48940 Leioa, Spain
[c] Ikerbasque, Basque Foundation for Science, 48009 Bilbao, Spain

ARTICLE INFO

Keywords:
Photocrosslinking
Hydrogel
Self-healing

ABSTRACT

Biocompatible and biodegradable hydrogels with biomimetic properties, such as self-repairing, are increasingly interesting for biomedical applications, particularly when they can be printed or *in situ* formed to mimic extracellular matrix or as personalized implantable devices in tissue regeneration or drug delivery. Photocrosslinkable hydrogels based on methacrylated chitosan (CHIMe) and hyaluronic acid that exhibit according with their composition, tuneable physico-chemical properties are here presented. The study of the conversion, gelation time, mechanical and rheological properties of photopolymerized CHIMe showed an optimal phenyl-2,4,6-trimethylbenzoylphosphinate (LAP) initiator feed (0.1 % w). These photocrosslinkable hydrogels demonstrated being able to promote doubly crosslinked hydrogels with similar Young Moduli regardless the cycles of self-healing processes, and tailored swelling (25–70 swelling factor), mechanical (1×10^{-4}-2×10^{-2} MPa) and rheological properties, as a function of polysaccharides relative content. Clear evidences have been found that fast photopolymerization of CHIMe/HA solutions leads to biocompatible (>80 % cell viability), biodegradable (20–24 days in hydrolytic medium) and robust self-healable hydrogels suitable for advanced biomedical and tissue engineering applications.

1. Introduction

The polymerization of monomers or polymers by ultraviolet (UV) and visible light has been investigated as an interesting approach for the development of *in situ* gelling hydrogels for drug delivery, biosensing and tissue engineering applications [1,2]. Macromers aqueous solutions act as injectable materials, remaining in liquid state before applying the light source and, becoming photopolymerized or photocrosslinked hydrogels after exposure to UV–visible light in a specific wavelength, due to an *in situ* curing process. Overall, among the different types of photopolymerization reactions, free-radical-initiated chain polymerization is the most used method in the biomedical field [3].

In free radical photopolymerization processes, the photoinitiator absorbs light photons, which promote their cleavage and, consequently, highly reactive free radical moieties are formed. Then, free radical moieties are able to react with vinyl groups present in the monomers (or vinyl modified polymers), leading to covalently crosslinked 3D networks. Several radical photoinitiators have been proposed for bioapplications, being 2-hydroxy-4′-(2-hydroxyethoxy)-2-methyl-propiophenone (Irgacure 2959) the most used [4]. However, its low water solubility and the need to use ultraviolet light of 365 nm are its main limitations, as exposure to light in this range may have harmful consequences for cells and tissue [5]. Therefore, photoinitiators that work in wavelengths near or in the visible range have been also developed. In this line, lithium phenyl-2,4,6-trimethylbenzoylphosphinate (LAP), a blue light photoinitiator stands out, since it has demonstrated high water solubility, high biocompatibility and allows good cell encapsulation when low concentration and longer light wavelengths are used (365–405 nm) [4].

Photocrosslinkable solutions are typically based on acrylated derived polymers that polymerize and crosslink *via* chain growth mechanism [6]. In this sense, the most studied photopolymerized polymers in recent years are those derived from modified biocompatible polymers, such as acrylate or methacrylated poly(ethylene glycol) (PEG) [7] or modified

* Corresponding author.
E-mail address: leyre.perez@ehu.es (L. Pérez-Álvarez).

https://doi.org/10.1016/j.ijbiomac.2022.07.004
Received 11 May 2022; Received in revised form 16 June 2022; Accepted 1 July 2022
Available online 5 July 2022

natural polysaccharides, for example, methacrylated dextran [8], methacrylated hyaluronic acid [2] or methacrylated chitosan [9].

Indeed, there are numerous promising polymers for the development of photocrosslinkable hydrogels, however, chitosan stands out above the rest due to its promising physicochemical and cell adhesion properties [10]. Chitosan is a naturally occurring weak polycation (pKa = 6.5) that it is formed by randomly ordered *N*-acetyl-glucosamine and glucosamine units. Chitosan is biocompatible, mucoadhesive [11], biodegradable and due to its cationic nature it presents antibacterial activity [12]. In addition to good biocompatibily and biodegradability, the large number of free amino groups present along its backbone facilitates its chemical modification with photocrosslinkable groups. Thanks to these features, its use in biomedical applications, such as *scaffolds* for tissue engineering [2] or drug delivery systems [13,14] has increased over the last decades. The chemical conjugation of chitosan with photopolymerizable groups has been carried out using different chemical reactions in order to obtain photocrosslinkable *in situ* forming hydrogels [15]. This is the case of Kolawole et al. [16], showing the development of methacrylated water soluble chitosan (methacrylated glycol chitosan) to prepare photocrosslinkable hydrogels that demonstrated great potential for the treatment of bladder cancer.

Chitosan has been chemically modified also by styrenation and then, polymerized by visible light exposure employing camphorquinone photoinitiator. Yu et al. [17] in addition to styrenized chitosan, also included biopolymers such as heparin, gelatin or hyaluronic acid, previously modified with different vinyl groups for the preparation of different photocrosslinkable chitosan-based hydrogels [17].

Hyaluronic acid is a weak polyanion (pKa = 2.9) composed of two repetitive disaccharide units: *D*-glucuronic acid and *N*-acetyl-*D*-glucosamine. This natural polysaccharide is mainly found in the extracellular matrix of animal tissues and its main characteristics are high hydrophilicity and biodegradability. We previously reported that the combination of CHI and HA is particularly interesting for biomedical applications due to the ability for self-healing of the obtained polycomplex hydrogels (CHI/HA) [18]. Self-healing, provides the material with the ability to repair damage on its own, restoring bonds or interactions after they have been disrupted, due to their reversible nature. Among the different types of reversible bonds/interactions [19], electrostatic interactions are the most simple and used ones for the development of self-healable hydrogels. This self-repairing ability leads to longer shelf-life of biomaterials while reducing replacement costs and consequently, the development of hydrogels with this capability has aroused great interest [20].

As previously mentioned, partially methacrylated chitosan presents unmodified primary amine groups that ionize at a suitable pH (pH < pKa) forming a polycation, which ideally would electrostatically interact with polyanions, such as carboxymethyl cellulose, alginate or hyaluronic acid [18].

In this context, biocompatible, biodegradable, photocrosslinkable, *in situ* forming and self-healable hydrogels could be prepared based on these two polysaccharides, namely methacrylated chitosan and hyaluronic acid. So far, few studies have investigated the properties of the direct mixture of chitosan and hyaluronic acid [21,22] and to the best of our knowledge, there is no information on the combination of electrostatic interactions between hyaluronic acid and photocured methacrylated chitosan hydrogels. Methacrylated chitosan has been exploited in the last years as printable hydrogel ink alone [23] or in combination with other polysaccharides, typically gelatin [24], and always different to hyaluronic acid. Taking this into account, this work aims to develop self-healable and photocurable chitosan hydrogels electrostatically crosslinked with hyaluronic acid and to explore the possibility of the self-healing ability in these kind of doubly crosslinked networks. This potential ability makes the difference with previously reported investigations on photocrosslinkable hydrogels of these polysaccharides [24,25]. Thus, the modification of chitosan through methacrylation and its subsequent photo-curing process with and without hyaluronic acid have been here deeply studied by FTIR and Photo-DSC. The synthesized CHIMe/HA hydrogels were characterized in terms of mechanical stability, rheological properties, morphology, swelling and degradation, properties that are highly influenced by hydrogel composition. Prepared hydrogels remain the potential ability to self-repair that was demonstrated by mechanical and rheological analysis, as well as their biocompatibility. These properties make them excellent candidates for acting as drug or cell carriers and scaffolds, being useful in tissue engineering, wound dressing and biomedical applications.

2. Materials & methods

2.1. Materials

Hyaluronic acid (Contipro, high molecular weight, $2.1 \times 10^6 \pm 1.01 \times 10^5$ g/mol (PDI = 1.003)) and chitosan from crab shells (Sigma Aldrich, highly viscous, $8.7 \times 10^5 \pm 4.0 \times 10^4$ g/mol (PDI = 1.037), deacetylation degree of 85 % ##determined by ^{1}H NMR) were used for the formation of photocrosslinkable hydrogels. The average molecular weights were measured by gel permeation chromatography using a PolySep-GFC-P Phenomenex column (Linear 300 × 7.8 mm) and as eluent 0.05 M (for hyaluronic acid) and acetic acid 0.15 M (for chitosan) (1 mL/min flow). The photoinitiator lithium phenyl-2,4,6-trimethylbenzoylphosphinate (LAP), acetic acid (for analysis, ≥ 99.8 %), sodium phosphate monobasic (≥ 99.0 %), sodium hydroxide (pure, pharma grade), methacrylic anhydride, deuterium oxide (99.9 % atom D), acetic acid-d_4 (≥99.5 % atom D), lysozyme (from chicken egg white, ~70,000 U/mg) and hyaluronidase (from sheep testes, type II, lyophilized powder, ≥300 units/mg solid) enzymes were purchased from Sigma Aldrich.

2.2. Preparation of photocrosslinkable hydrogels

2.2.1. Modification of chitosan polysaccharyde

Pristine chitosan (CHI) was modified by reaction with methacrylic anhydride (MA) at different molar equivalents in order to generate photocrosslinkable chitosan with different degrees of modification (Table 1) [16].

Briefly, 1.5 % *w*/w chitosan solution was prepared by dissolving the corresponding chitosan amount in a 0.5 % *v*/v acetic acid solution at room temperature for 12 h. Then, different volumes of methacrylic anhydride (1:1, 1:10, 1:20 and 1:100) were added dropwise to the solution protected by light maintaining constant magnetic stirring at 40 °C during 24 h. In addition, for CHI:MA 1:20 M different intervals of time (1, 24, 48 and 72 h) were also established. The remaining product was purified by exhaustive dialysis (12–14 kDa membranes) for 4 days and lyophilized at −50 °C and 0.1 mBar.

2.2.2. Synthesis of photocrosslinkable hydrogels

Separate solutions of methacrylated chitosan (CHIMe, 1:20 CHI: Methacrylic anhydride feed ratio and 24 h) and hyaluronic acid, both at a concentration of 1.5 % (*w*/w) were prepared in 0.5 % (*v*/v) acetic acid solution. The viscosities of the prepared solutions were 7260 ± 240 cP for methacryled chitosan and 34,520 ± 479 cP for hyaluronic acid, measured with a Brookfield DV2T *v*iscosimeter. The corresponding amount of LAP photoinitiator was previously dissolved in a minimum amount of acetic acid 0.5 % (*v*/v) (500 μL approximately) and added to methacrylated chitosan solution that was then mixed with the prepared

Table 1
Weight percentages for the preparation of CHIMe/HA hydrogels.

% CHIMe (*w*/w)	% HA (w/w)	% LAP (w_{LAP}/w_{total})
100	0	0.01; 0.05; 0.1; 0.2; 0.5
70	30	0.01; 0.05
50	50	0.01; 0.05

HA solution in different weight ratios (Table 1). After vigorous stirring, the mixture was placed at 1.5 cm under UV light LEDs (385 nm, 19 mW/cm^2) and hydrogels were formed *in situ*.

2.3. Physical-chemical characterization of CHIMe/HA hydrogels

2.3.1. Gelation time

Gelation time of the aforementioned hydrogels were determined using the inverted tube test [26,27]. The gelation time of the hydrogels was studied at different photoinitiator percentages ranging from 0.01 to 0.5 (Table 1, three replicates were employed).

2.3.2. Nuclear magnetic resonance (^{1}H-RMN)

The degree of methacrylation of chitosan was determined by NMR spectroscopy. Briefly, ^{1}H NMR spectra were taken in D_2O acidified with acetic acid-d_4 at a concentration of 0.5 % *v*/v on a Bruker Avance 500 MHz spectrometer at 25 °C employing a polymer concentration of 1.5 % *w*/w. According with literature [16], the methacrylation degree (MD) was calculated based on the ratio of the relative integrals area of the H2-H6 protons of *N*-acetyl-glucosamine units of chitosan and the resonance peaks of methacrylate groups at 5.6 and 6.2 ppm (see Eq. (1)):

$$\mathrm{MD}\ (\%) = \frac{(\text{Integral of methacrylate protons at } 5.6 - 6.2 \text{ ppm})/2}{(\text{Integral of chitosan cycle protons at } 2.8 - 3.9 \text{ ppm})/6} \times 100 \quad (1)$$

Shown data correspond to the average of three samples.

2.3.3. Fourier-transform infrared spectroscopy (FTIR)

FTIR spectra of pristine polysaccharides and dried hydrogels were registered by a Nicolet Nexus FTIR spectrometer (Thermo Scientific). The experiments were carried out using KBr pellets in the case of the pure polymers and ATR in the case of modified polysaccharides and hydrogels (4 cm^{-1} resolution and 32 scans).

2.3.4. Photo-differential scanning calorimetry (photo-DSC)

The UV curing process was studied by photo-DSC, using a DSC (TA Instruments Q2000) equipped with a photocalorimetric accessory (Omnicure S2000) which presents a 200 W mercury lamp, an optical range from 320 to 500 nm and an intensity between 1 and 2 mW/cm^2. The sample area in all cases was 0.2 cm^2.

According to the literature [28] the conversion degree (α) of double bonds (C=C) can be obtained considering the area of the exothermic peak during light induced reaction and using Eq. (2).

$$\alpha = \frac{\Delta H_t}{\Delta H_0^{theor}} \quad (2)$$

where ΔH_t (J/g) is the reaction enthalpy at time t, and ΔH_0^{theor} (J/g) is the theoretical value of the enthalpy for the complete conversion, calculated following Eq. (3).

$$\Delta H_0^{theor} = \frac{54.7 \times \text{Functionality}}{M_w^{theor}} \quad (3)$$

ΔH_w^{theor} is the molecular weight of pristine chitosan, 54.7 kJ/mol is the molar enthalpy of the methacrylate group and functionality is 1 in the present case.

2.3.5. Morphological characterization

The morphology and the pore size of the hydrogels were studied using a Hitachi S-4800 scanning electron microscope (SEM), (150 s, 20 mA, 15 kV, ×30,000 magnification). CHIMe/HA hydrogels were first lyophilized (−50 °C, 0.1 mBar) and then coated with gold.

2.3.6. In vitro swelling

Hydrogels were lyophilized at −50 °C and 0.1 mBar. Subsequently, they were immersed in phosphate buffer solution (PBS) (pH = 7.4) at 37 °C in order to imitate physiological conditions. The swelling ratio was measured over time and the swelling factor was calculated according to Eq. (4):

$$\text{Swelling factor} = \frac{W_s - W_d}{W_d} \quad (4)$$

where, W_s and W_d are the weights of the swollen and dried hydrogels, respectively.

2.3.7. Rheology

The dynamic rheological measurements of CHIMe/HA photo-crosslinkable hydrogels were performed through a Rheometric Scientific Advanced Rheometric Expansion System (ARES) using a parallel plate geometry (25 mm of diameter and separated 1.5 mm). The viscoeleastic limit was determined by a shear strain sweep and then, storage (G') and loss modulus (G") were measured at 25 °C varying frequency (0.1 to 500 rad/s at a fixed strain of 1 %). Both strain and frequency sweeps were measured in triplicate.

After subjecting the photocrosslinkable hydrogel to subsequent three cut-repair cycles (1 cycle = 1 cut +1 recovery), the rheological properties were also studied following the method described above.

Strep-strain test was also carried out measuring the storage and loss moduli of a hydrogel sample (CHIMe:HA 50:50 0.05 % LAP) at room temperature, fixing frequency at 1 Hz, during alternate cycles of 1 min, in which the hydrogel remained under strain below (0.1 %) and above (50 %) its deformation limit. This cut-recovery process was repeated 3 times.

2.3.8. Compressive stress/strain test

Compression stress/strain tests were performed in an Metrotec FTM-50 texture analyzer using a 20 N load cell. Measurements were made with a compression rate of 1 mm/min until failure. Compression moduli were calculated from a linear regression on the strain-stress curves between 40 and 60 % strain.

On the other hand, compression stress/strain tests were also carried out in self-healed hydrogels after increasing cut-recovery cycles (1–3). For this, samples were cut in two pieces that were put together at room conditions and instantaneously healed.

2.4. Functional characterization

2.4.1. In vitro biodegradation

Freshly prepared CHIMe/HA hydrogel were immersed in phosphate-buffered saline solution at pH 7.4 at 37 °C. The mass loss along the time was registered as a quantification of the *in vitro* hydrolytic biodegradation (Eq. (5)):

$$\text{Mass loss}\ (\%) = 100 - \left(\frac{W_0 - W_t}{W_0} \times 100\right) \quad (5)$$

where W_0 is the weight of the multi-crosslinked hydrogel at initial time and W_t at t_∞. Three samples were evaluated for each data point.

The enzymatic degradation was carried out as described above, but immersing hydrogels in 2 different enzymatic media: lysozyme or hyaluronidase at a concentration of 1 mg/mL.

2.4.2. In vitro cytotoxicity assay

Live/dead assay (ThermoFisher) was carried out with prepared hydrogels and employing mouse embryonic fibroblasts (MEFs). These cell were plated in a 24-well plate at a density of 2.10^5 cells/well, and cultured following standard conditions (37 °C and 5 % CO_2) in a complete medium (DMEM with 10 % fetal bovine serum and 1 % penicillin). The next day, CHIMe/HA hydrogels (5–10 mg) were sterilized under UV light for 1 h after being washed with D-PBS and dried, and finally added to the wells. Hydrogels were removed after 24 h and the cell cultures were washed with PBS and stained with Calcein-AM (2 μM), ethidium

homodimer (EthD-1, 4 μM) and NucBlue (Thermo Fisher R37605, 2 drops/well). Fluorescence images of the blue (NucBlue), green (Calcein) and red (EthD-1) channels were acquired using a Leica DMi8 microscope. Quantification of cell survival, calculated as the ration between red-stained and blue stained nuclei, was performed using Fiji software [29].

2.5. Statistical analysis

Numerical data shown as mean ± standard deviation were conducted with a minimum of $n = 3$. Statistical significance was determined by one-way analysis of variance (ANOVA) and Tuckey tests, using the OriginLab 9.1 software. Significance was defined for $p < 0.05$.

3. Results & discussion

3.1. Optimization of methacrylation process

The chemical modification of pristine chitosan was carried out using a single reaction with methacrylic acid. As illustrated in Fig. 1A, the characteristic primary amine moieties ($-NH_2$) of chitosan react with the carbonyl group of methacrylic anhydride by nucleophilic attack, which, as a result, leads to the formation of a new amide bond. To corroborate and quantify the introduction of the methacrylic group in the polysaccharide, FTIR and ^{1}H NMR analyses were performed.

Infrared spectra (Fig. 1B) of chitosan and modified chitosan evidence that the modification of chitosan to form photocurable polysaccharide takes place successfully. Regarding chitosan spectrum, the bands appearing at 1662 cm^{-1} and 1595 cm^{-1} are identified, which correspond to amide I and amide II bands, respectively. In the same line, the twisting of CH_2 and C—N stretching at 1418 cm^{-1} and 1322 cm^{-1} can be also observed. Accordingly, the overlaying of the spectra of pristine chitosan and methacrylated chitosan shows that the latter has the same characteristic bands, and at 1615 cm^{-1} a new band is also observed, which corresponds to the stretching of C═C double bands resulting from the methacrylation process [9].

Further, in the ^{1}H NMR spectra of chitosan (Fig. 1C) the signal corresponding to the methyl protons of the acetyl group of chitosan can be distinguished at 2 ppm, as well as the representative peaks of protons from the glucosamine ring between 2.8 and 3.9 ppm and the signal of the proton of the deacetylated part at 2.8 ppm. Additionally, regarding the ^{1}H NMR of the methacrylated chitosan, some additional peaks can be observed, corroborating the modification reaction. This is the case of the signals that appear at 5.6 and 6.2 ppm, which correspond to the hydrogens of the double alkenyl bond from the methacrylate moiety conjugated to chitosan. Moreover, an additional peak at 1.85 ppm is also observed, corresponding to the protons of the $-CH_3$ moiety of the methacrylic groups. These spectral data are in good agreement with those reported in the literature [16,17]. The degree of modification can be quantified by the integration of the resonance signals of the four protons of the -C=C- bonds (5.6–6.2 ppm) with respect to the broad resonance band of the glucose ring from 2.8 to 3.9 ppm.

The modification of chitosan was carried out varying the molar equivalents of the methacrylic anhydride with respect to the chitosan and the reaction time (Fig. 2). High values of methacrylation degree are preferred for photocrosslinking reactions in order to develop photocrosslinkable *in situ* forming hydrogels. However, methacrylation degree also influences a wide variety of properties, including mechanical and rheological properties and swelling, among others, that in turn, influence the processability and applicability of the hydrogels.

Fig. 2 shows the influence of adding molar equivalents of methacrylic anhydride and methacrylation times on the methacrylation degree (MD). Up to 1:10 CHI:Methacrylic anhydride feed ratio, the methacrylation degree does not show a significant variation. Similarly, modification degree remains almost invariable after 24 h of reaction. Therefore, it was concluded that the reaction conditions that lead to the highest MD in the shortest time correspond to 1:20 CHI:Methacrylic anhydride feed ratio and 24 h reaction time. These conditions were used for the following studies.

3.2. Optimization of the photopolymerization process of CHIMe

The radical photoinitiator lithium phenyl-2,4,6-trimethylbenzoylphosphinate (LAP) has attracted great interest in recent years due to its high biocompatibility, and high molar extinction coefficient, which increases polymerization rate with light absorption capacity allowing rapid polymerization with visible light in the range of 365–400 nm.

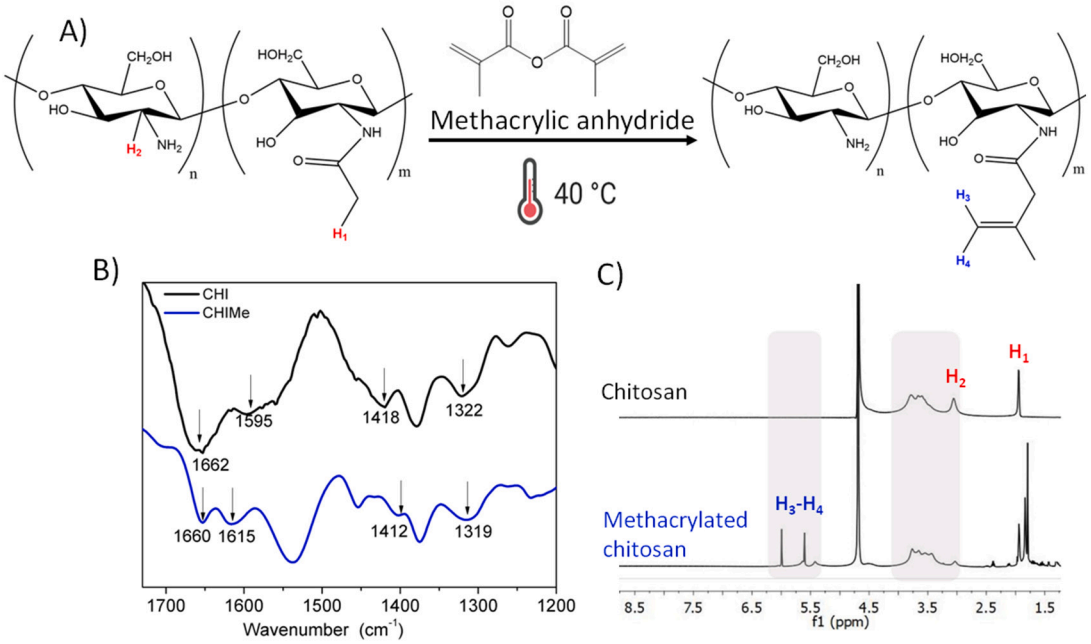

Fig. 1. A) Reaction scheme for the synthesis of methacrylated chitosan, B) FTIR and C) ^{1}H-NMNR spectra of unmodified and modified chitosan.

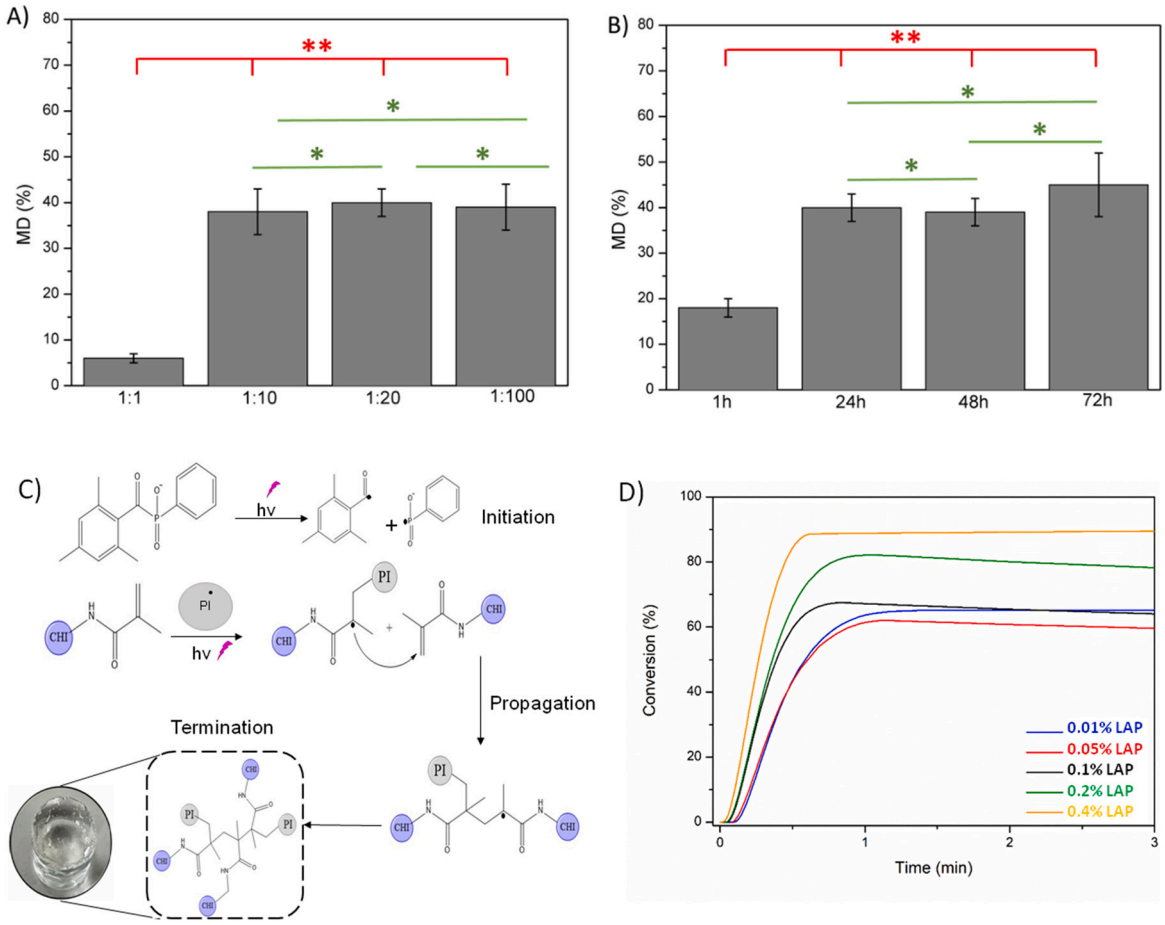

Fig. 2. A,B) Influence of A) CHI:Methacrylic anhydride feed ratio (24 h) and B) Reaction time on the methacrylation degree of chitosan (1:20) (^{1}H NMR determined). One-way ANOVA test with Tukey's multiple comparison test was used for the statistical analysis ($p < 0.05$). (*) No significant differences and (**) significant differences C) Methacrylated chitosan-based hydrogels' photopolymerization process scheme and D) Curing conversion (α) of CHIMe/LAP hydrogels.

Photopolymerization begins by irradiating the sample composed of LAP and CHIMe with light of 385 nm (Fig. 2C). This light is absorbed by LAP molecules in the mixture, causing their dissociation into two radicals. Subsequently, the free radicals attack the C═C group of the methacrylated chitosan, initiating the photopolymerization of the modified polysaccharide. Finally, a three-dimensional polymeric structure based on the crosslinking of the polymeric chains of methacrylated chitosan is obtained [30].

For the characterization of the photopolymerization process of CHIMe, different concentrations of photoinitiator have been used in order to study the influence of LAP on the physicochemical properties of the prepared hydrogels. As presented in Fig. 2D, an increase in LAP content produces an increase in the conversion degree of the hydrogel, varying from nearly 60 % in the case of the 0.01 % of LAP to 90 % in the case of 0.4 % of LAP. Conversion degree can be considered indicative of the crosslinking efficiency in the gels, being higher than 50 % in all the cases. In addition, t_{max} decreases considerably when photoinitiator content increases.

Gelation times for the compositions with varying LAP concentrations were determined by the inverted vial method when they are at 5 mm from the 385 nm LEDs (Fig. 3A). Furthermore, rheological and mechanical properties of the CHIMe/LAP hydrogels were evaluated by frequency sweep and stress-strain test respectively, to investigate also the effect of photoinitiator content in the properties of chitosan-based hydrogels, as presented in Fig. 3B and C.

A variation in the percentage of photoinitiator results in a noticeable variation in the gelling time of the gels (Fig. 3A) determined by the inverted tube test. The increase in the concentration of photoinitiator promotes the formation of free radicals, which, in turn, are responsible of guiding the photo-crosslinking process in order to achieve 3D hydrogels. As shown in Fig. 3A, an increase in LAP concentration (from 0.01 % to 0.4 %) causes a 4-fold decrease in the gelation time which is a key factor since, as mentioned previously, it limits the precision of the printing process.

Rheological results suggest (Fig. 3B) that all samples show gel-like behaviour since the values of the storage moduli are higher than loss moduli values in all frequency range ($G' > G''$). This behavour indicates that elastic properties of the analyzed materials predominate over the viscous ones, which is the typical behaviour of hydrogels. Collected data demonstrate that covalent network based on CHIMe/LAP are formed even with the lowest photoinitiator content (0.01 %). However, different values of the storage modulus were obtained for the prepared hydrogels which reveal a clear dependence of the rheological properties as a function of the concentration of the photoinitiator. In this sense, an increase in photoinitiator content in methacrylated chitosan/LAP hydrogel composition leads to an increase in the value of the storage modulus. As a result, the hydrogels prepared with a larger amount of photoinitiator (0.4 %) are also those that have larger storage moduli being 12 times greater than in the case of hydrogels that have a low content of LAP (0.01 %). It is important to note that although in Fig. 3 it is evident that the gels with 0.01 % LAP are those that present the weakest rheological properties, as the photoinitiator content increases, the difference between G' values becomes smaller.

On the other hand, the influence of LAP concentration in the compression properties of the hydrogels is shown in Fig. 3C. It is observed that the compression deformation increases nonlinearly when

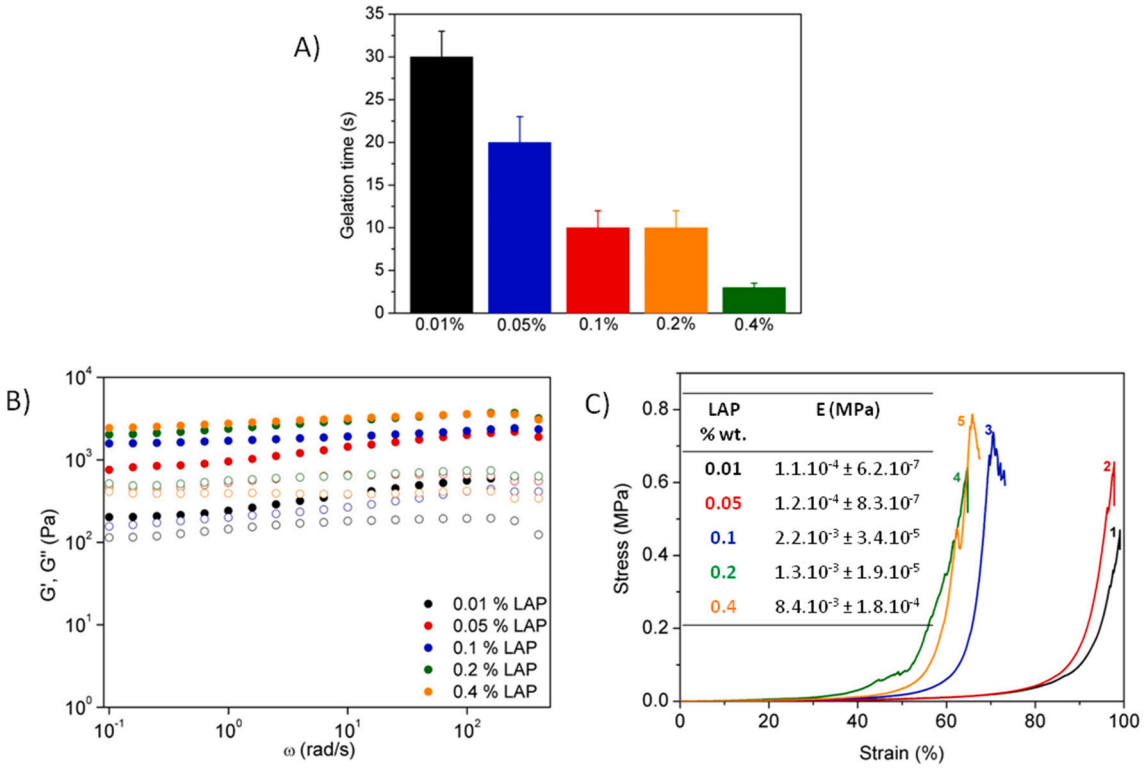

Fig. 3. Influence of LAP content (%) in A) Gelation time, B) Storage modulus (G', filled circles) and loss modulus (G", open circles) of the prepared hydrogels in a frequency scan and C) Mechanical stability under compression stress/strain tests.

increasing compression stress, which is a typical non-linear behaviour of hydrogels. In addition, the gels with a lowest content of photoinitiator (0.01 %) are the softest hydrogels with fewer crosslinking points, increasing the percentage of LAP in the gel content, a strong increase can be observed in the mechanical stability of the hydrogels, making the hydrogels more rigid. In the case of the highest LAP concentrations (0.1, 0.2 and 0.4 %) very similar mechanical properties were measured, that is in line with rheological data (Fig. 3B). These results and the potential use of these hydrogels as smart inks for applications in the biomedical area determine the optimum LAP concentration. Hence, higher quality printing is promoted with inks that become hydrogel as rapid as possible to prevent spreading. On the other hand, the presence of unreacted free radicals that are susceptible of being cytotoxic limits optimal LAP concentration [5]. Therefore, taking all this into account, LAP percentages of 0.05 and 0.1 are selected for the following tests as they offer fast and intermediate gelation times (20 and 10 s, respectively), as well as good mechanical and rheological properties, not very different from those gels with a higher percentage of photoinitiator.

3.3. Synthesis and characterization of self-healable photocrosslinkable hydrogels

Hydrogels with the ability to autonomously self-repair are highly interesting for a variety of applications and can be designed according to different properties in order to allow the repair process of the damage structure in the desired scale of time while maintaining mechanical integrity, among others. Despite polysaccharides are interesting candidates, their self-healing ability is restricted to the presence of active functionalities that promote reversible and strong interactions. Photopolymerized methacrylate chitosan hydrogels are based on non-dynamic covalent bonds that were repeatedly established between the crosslinking by the introduced methacrylic moiety on chitosan. Accordingly, once these links are damaged, they are irreparable due to their permanent and non-reversible nature. Therefore, to achieve the self-healing capacity, it is necessary to add some functionality that interacts with elements of the formed network (Fig. 4A), such as the remaining unmodified primary amine groups of chitosan. According to the ^{1}H-RMN spectra of Fig. 1B, the unmodified –NH_2 are about 60 % of the initial amounts of free amines in chitosan. These moieties confer to chitosan the ability to interact by electrostatic interactions, among others, with polyanions. This is the case of hyaluronic acid that has been incorporated to the previous formulation at varying CHIMe:HA ratio (70:30 and 50:50), as is described in the experimental section. The electrostatic interactions between these two natural polysaccharides together with the covalent crosslinks between methacrylate moieties results on the *in situ* formation of doubly crosslinked photocurable hydrogels (Fig. 4A). Electrostatic interactions between the carboxylate group (-COO^-) of hyaluronic acid and amine (-NH_3^+) of chitosan were favoured by adjusting the pH at an intermediate value between hyaluronic acid and chitosan pKa value, 2.9 and 6.5, respectively [31], in which ionization of both polymers is maximum. The photocurable hydrogels were prepared varying polysaccharides concentration (Table 1) and using the LAP concentrations selected in the previous section, 0.05 and 0.1 %, in order to optimize complexation and self-healing ability.

Fig. 4B shows the FTIR spectra of pure hyaluronic and methacrylated chitosan, as well as the photocurable polyelectrolyte complex hydrogel formed by mixing upon UV light. As indicated before, the characteristic peaks of methacrylated chitosan appear at 1662 cm^{-1} and 1595 cm^{-1}, which correspond to amide I and amide II bands. In the same line, the absorption band of C═C appears at 1615 cm^{-1} indicating the presence of methacrylated groups. Hyaluronic acid also shows amide I and amide II bands and C—N stretching at 1671 cm^{-1} and 1555 cm^{-1}, respectively. Furthermore, the asymmetric and symmetric stretching of carboxylate group appears at 1620 cm^{-1} and 1415 cm^{-1}, and the stretching of C—N at a wavenumber of 1320 cm^{-1}. Regarding FTIR spectrum of the formed photocurable complex, a slightly shifted wide band with respect to the original polymers is observed between 1660 and 1600 cm^{-1} which correspond to the overlapping of amide I bands of hyaluronic acid and

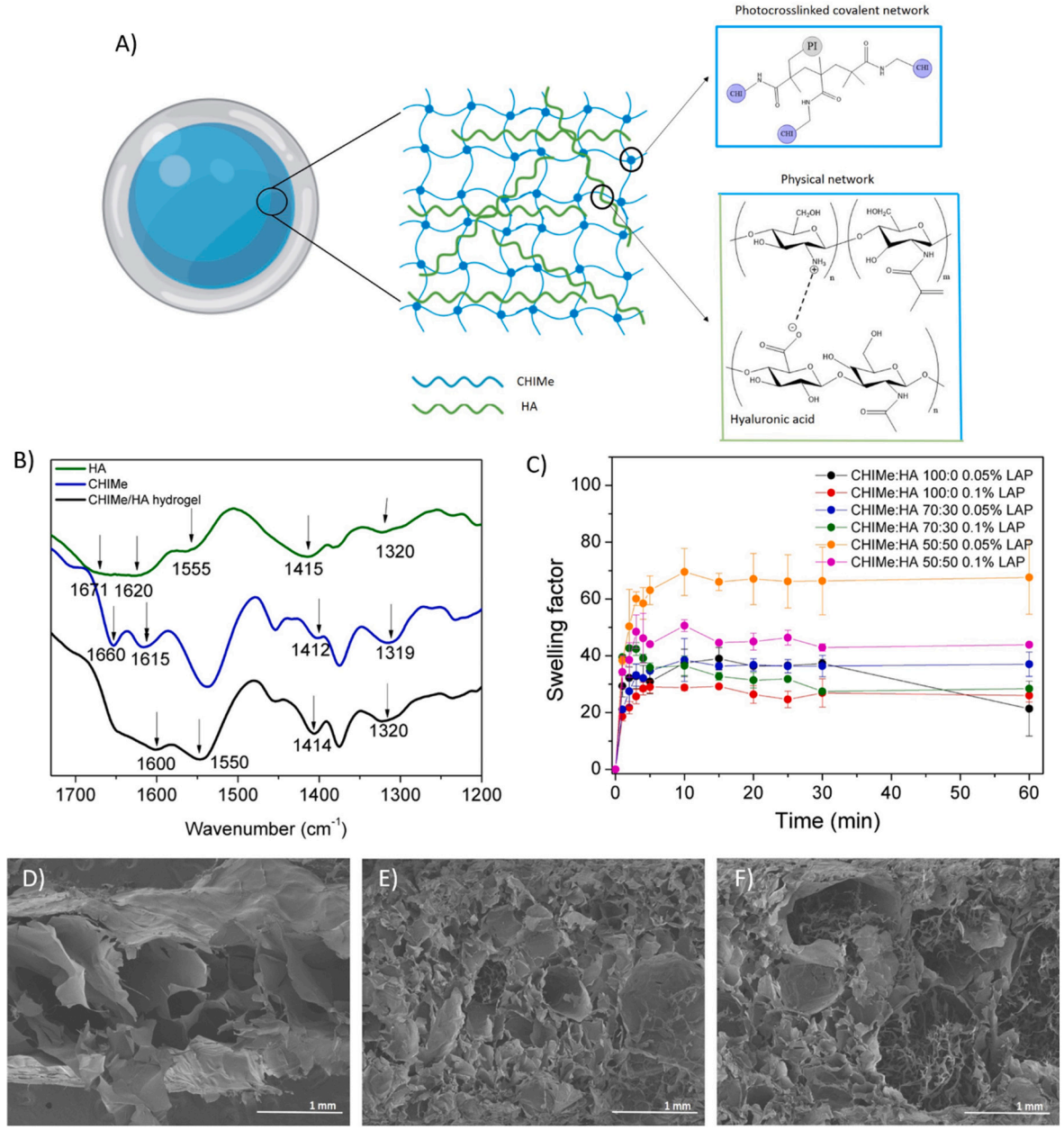

Fig. 4. A) Schematic representation of the formation of methacrylated chitosan/hyaluronic acid-based photocrosslinkable and self-healable hydrogel. B–D) SEM images of CHIME:HA B) 100:0 0.05 %, C) 70:30 0.05 %, D) 50:50 0.05 % E) FTIR spectra of pure hyaluronic acid, methacrylated chitosan and photocrosslinkable hydrogel and F) Swelling behaviour of the different photocrosslinkable hydrogels.

methacrylated chitosan. According to literature [31,32], this slight shifting of amide bands can be ascribed to the electrostatic interactions between two polysaccharides, which suggests that the complexation has taken place. Further, around 1414 cm^{-1} and 1320 cm^{-1} the characteristic two bands that correspond with the symmetric stretching of the carboxylate group of hyaluronic acid and C—N of methacrylated chitosan are also present [33,34]. Finally, the disappearance of the characteristic absorption band of the C═C group of methacrylated chitosan at 1620 cm^{-1} is another evidence that in addition to the complexation between the two polymers, the photopolymerization process has taken place successfully.

Due to the double crosslinking, that combines both physical interactions and covalent bonds, macroscopic networks are formed *in situ* giving rise to porous materials in all cases, in good agreement with the literature [18] (Fig. 4D–F). The prepared networks, which are similar to those characteristic of physical and covalent hydrogels, show a clear dependence of the morphology with the composition of the hydrogels, showing that the introduction of hyaluronic acid to CHIMe-based hydrogels strongly increases the crosslinking density together with the decrease of the pore size (Fig. 4D-F). Swelling factor (at physiological pH and temperature) of the hydrogels prepared at different photoinitiator (0.05 and 0.1 % *w*/w) and polysaccharides contents (0–100 % w/w) are shown in Fig. 4C. The swelling of the different hydrogels demonstrate that it depends considerably on the photoinitiator and the photocurable CHIMe content. The swelling factor of all samples decreases when 0.1 % of LAP was used in comparison with 0.05 % content. A higher amount of LAP (0.1 %) favours the photopolymerization process, which results in a higher number of crosslinking points that lead to smaller pores in the network, limiting water absorption. On the other hand, increasing the concentration of methacrylated chitosan (from 50 to 100 %), thus, decreasing the concentration of hyaluronic acid, leads to a lower swelling factor in all the samples with the same LAP content. This

suggests that the covalent crosslinking predominates over the physical one. In the same line, a higher percentage of chitosan, that leads to covalent crosslinks in the hydrogel, results in lower pore sizes, a more compact structure and lower swelling factors. It is also important to highlight that the swelling does not only depend on the crosslinking density of the hydrogel. In fact, pore size is one of the most influential factors in swelling, however, it is not the only one. The addition of hydrophilic molecules, such as hyaluronic acid which is one of the most hydrophilic molecules in nature [35], in addition to leads to a higher crosslinking density, also increases the hydrophilicity of the material and, therefore, it leads to a larger ability to absorb water [36], which implies opposite effects.

On the other hand, Fig. 5A shows the results obtained from the rheological measurements. In all cases, the value of G' is larger than that of G″, which indicates a typical behaviour for hydrogels. Further, it is important to highlight the influence of the composition on the rheological behaviour of the material. The samples containing the highest amount of chitosan (CHIMe:HA 100:0 0.05 and 0.1 % LAP), which were also the hydrogels with the lowest swelling capacity, shown higher G' values. Indeed, a decrease in chitosan content, this is, an increase in hyaluronic acid content, promotes the formation of a larger number of physical bonds that reduces the possibility of developing covalent bonds, which results in a deterioration of the rheological properties. Nevertheless, it is noticeable that differences are larger between the compositions 100:0 and 70:30, than when the ratio was decreased from 70:30 to 50:50. This effect can be ascribed to the substitution of CHIMe by hyaluronic acid in the feed, leading to a reduction of covalent linkages in the network but, at the same time, to an additional electrostatic crosslinking that is more noticeable when high HA content is incorporated (50 %).

Fig. 5B shows the compression properties of the hydrogels, revealing that the compression modulus increases as the deformation increases, showing in all the samples the typical non-linear behaviour of hydrogels. On the other hand, and according to the rheological results, hydrogels based only in photocrosslinked chitosan (100:0 CHIM:HA 0.05 % LAP) are the most elastic ones. In all compositions, the increase of photoinitiator feed leads to more rigid networks and higher Young modulus, as well as lower strains at breakage. However, the addition of hyaluronic acid, on the one hand, promotes the formation of electrostatic interactions, but on the other hand, the loss of chemical crosslinking results in weakening the material and, therefore, leads to a decrease of the mechanical stability. These results are in line with the rheological results (Fig. 5A).

As previously mentioned, the healing mechanism of CHIMe/HA photocrosslinkable hydrogels is expected as a consequence of the association-dissociation process between ionized amine groups of chitosan and carboxylate groups of hyaluronic acid. Thus, in order to study the healing capacity of CHIMe/HA hydrogels, different hydrogels were synthesized in 30 s (longer photopolymerization time than the determined gelation times) and then were cut in two halves. Subsequently, two pieces were kept together and a few drops of water were added to facilitate the healing process. After 2 h all hydrogels were healed (Fig. 5C-F).

Rheological oscillatory analyses were also carried out in order to investigate the self-healing process of the CHIMe/HA hydrogels. For this, samples were healed after being cut into two halves and this process was repeated for three consecutive cycles. After each cycle, rheological and mechanical measurements were collected (Fig. 6).

As illustrated in Fig. 6A-D, G′ is higher than G″ after every cut-recovery cycle in every hydrogel regardless the composition thus, demonstrating the elastic properties for all hydrogels. Furthermore, the obtained data demonstrate a quick recovery of the viscoelastic properties of the broken CHIMe/HA hydrogels due to the electrostatic interactions based on the formation of polyanion-polycation bonds between the oppositely charged polysaccharides. As it can be observed in Fig. 6A-D, a slight loss of the storage modulus is observed in all cases

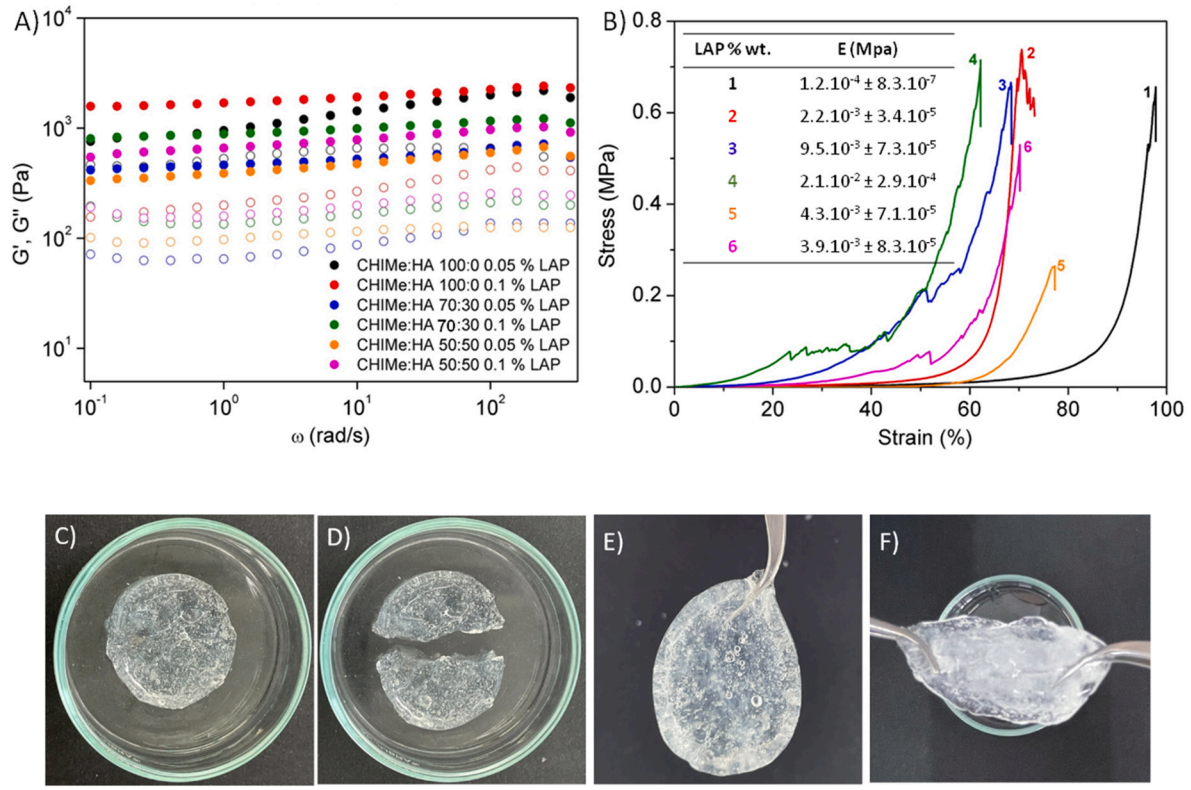

Fig. 5. A) Rheological properties of CHIMe/HA hydrogels in a frequency scan being G′ storage modulus (filled circles) and G″ loss modulus (open circles), B) Mechanical stability by compression stress/strain measurements and Self-healing process of hydrogels CHIMe:HA 50:50 with 0.05 % of LAP).

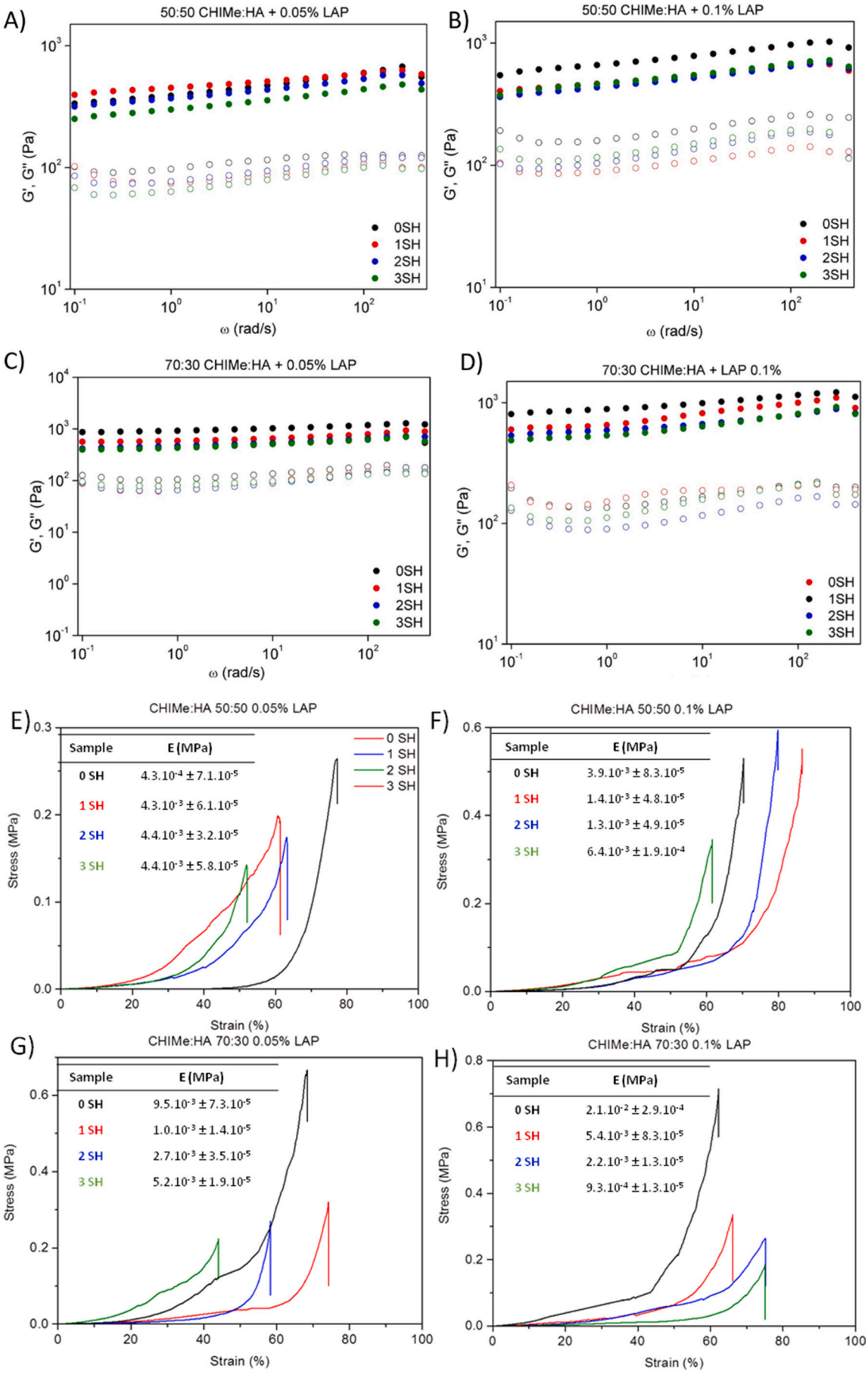

(caption on next page)

Fig. 6. Rheological results for A) 50:50 CHIMe with 0.05 % of LAP, B) 50:50 CHIMe with 0.1 % of LAP C) 70:30 CHIMe with 0.05 % of LAP and D) 70:30 CHIMe with 0.1 % of LAP after different cycles of cut-recovery (storage modulus G', filled circles and loss modulus G", open circles) and Compression stress/strain results for A) 50:50 CHIMe with 0.05 % of LAP, B) 50:50 CHIMe with 0.1 % of LAP C) 70:30 CHIMe with 0.05 % of LAP and D) 70:30 CHIMe with 0.1 % of LAP after different cycles of cut-recovery.

as the number of cycles of cut-recovery increases.

Further, the ability to self-repair was also evaluated by the evaluation of the mechanical stability of healed samples after different healing cycles (Fig. 6E-H). Compression tests show that, regardless the number of cut-recovery cycles, the deformability of the healed 50:50 CHIMe:HA 0.05 % LAP (Fig. 6E) hydrogel was slightly reduced (from 80 to ~60 % of breakage strain), and in the case of hydrogels with 0.1 % LAP (Fig. 6F), the deformability oscillates around that of the original hydrogel. However, as presented in Fig. 6 G and H, hydrogels based on 70:30 CHIMe:HA reveal a slight change in the stress required to be deformed, showing a larger impediment to recovering after being damaged. This fact could be ascribed to the fact that these hydrogels have larger amount of methacrylated chitosan in their composition, that is, more reactive moieties capable of photocrosslinking, increasing the mechanical stability of these materials. Furthermore, the composition of the hyaluronic acid in the hydrogels is slightly lower (~ 20 % *w*/w) which makes more difficult to establish the electrostatic interactions between two polysaccharides that are responsible for the mechanism of self-repair.

With respect to the Young Modulus, and independently of the number of healing processes, higher values (CHIMe:HA 50:50 0.05 % LAP) and similar values (CHIMe:HA 50:50 0.1 % LAP, CHIMe:HA 70:30 0.05 % and 0.1 % LAP) were obtained for repaired photocrosslinkable CHIMe:HA hydrogels in comparison with pristine networks. This is a typical behaviour of self-healable hydrogels mediated by electrostatic interactions between these two polysaccharides, according to the literature [18]. These results demonstrate the formation of a new material with suitable self-healing characteristics.

As expected, the typical behaviour of a gel G′ > G″ was inverted to that of a quasi fluid G″ > G′, when hydrogel sample (50:50 CHIMe with 0.05 % of LAP) was subjected to a strain above its deformation limit (50 %) (Fig. 7). However, the total inversion of the moduli, G′ > G″ was clearly observed when a deformation below the limit of the hydrogel was subsequently applied. Indeed, sample showed the ability to cyclically recover the typical behaviour of stable gels (G′ > G″) from that of the fluid or quasi-fluid (G″ > G′), corroborating the self-healing ability of the material.

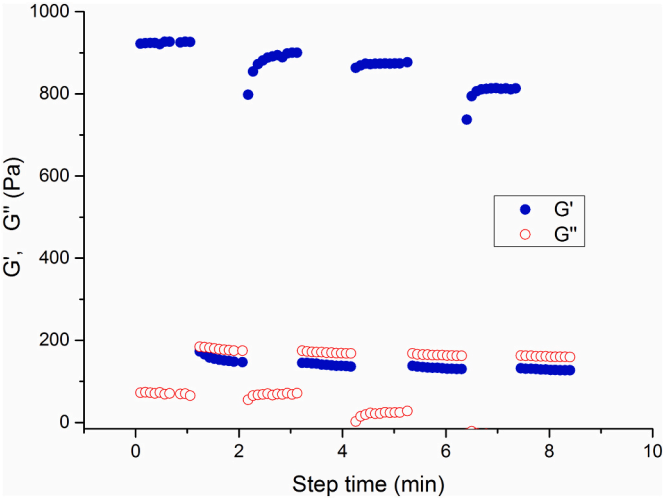

Fig. 7. Consecutive inversion of G′ and G″ during step-strain measurement alternating deformation cycles below-above-below the deformation limit of the gel at 1 Hz along the time.

3.4. In vitro hydrolytic and enzymatic biodegradation

The study of degradation kinetics is a key factor since it directly affects the stability of the materials and, therefore, its applicability in different areas such as controlled drug release or tissue engineering.

Thus, the hydrolytic degradation profile at physiological conditions (pH 7.4, 37 °C) of the gels is presented in Fig. 8. In addition, since the materials are based on two natural polymers, the degradation profile was also studied in enzymatic media for formulations with 0.05 % LAP. On the one hand, lysozyme was used because it is an enzyme specifically used to catalyze the biodegradation of chitosan through the hydrolysis of β-(1,4) glycosidic linkages [37,38]. On the other hand, hyaluronidase was also used because it favours the hydrolysis of the linkages between *N*-acetylglucosamine and glucuronic acid [39].

The collected data in Fig. 8A-D shown the hydrolytic degradations of the synthesized hydrogels. Initially, it could be observed that the hydrogels with a larger swelling capacity are also the ones more stable against degradation (50:50 CHIMe: HA 0.05 % LAP). However, as the degradation time increases, a clear trend is no longer observed, being all samples completely degraded at a similar same time of around 21 days. Nevertheless, the addition of enzymes demostrate a strong effect on the degradation kinetics of the photocurable hydrogels, leading to a faster degradation. In general, in the enzymatic medium and, unlike hydrolytic degradation, a clear tendency can be observed depending on the composition ([40]; [15]). In the case of lysozyme, an increase in chitosan content increases the speed of degradation. Thus, the hydrogels based solely on chitosan with 0.05 % LAP are completely degraded in 5 days. The same effect can be observed when hyaluronidase is used and the content of hyaluronic acid in the composition of the hydrogel is higher, since the number of bonds susceptible to hydrolysing increases, while the covalent bonds based on chitosan decrease. This explains that the degradation in hyaluronidase is faster for the 50:50 CHIMe:HA gels (0.05 % LAP) than for those containing 70:30 CHIMe:HA (0.05 % LAP).

3.5. In vitro cytotoxicity assay

To evaluate the toxicity of the hydrogels, a fluorescence-based cell viability assay has been carried out. Specifically, the survival rate of murine embryonic fibroblasts (MEFs) was evaluated after incubation with CHIMe:HA gels using two concentrations of LAP (0.05 % and 0.1 %). The ratio between cell nuclei stained with EthD-1 and those stained with NucBlue was used to determine the survival rate in each well. The results reveal no statistical differences between the groups (Fig. 8E, F), indicating a high biocompatibility of the CHIMe:HA gels, independently of the concentration of LAP used.

4. Conclusions

Photocrosslinkable hydrogels based on methacrylated chitosan and hyaluronic acidwith tailored, physico-chemical properties are here presented. Hydrogels based on CHIMe/HA show that lower photocrosslinkable chitosan content increases hydrophilicity and, therefore, endorsing hydrogels swelling, while mechanical and rheological properties, however, are improved increasing covalent crosslinking for high CHIMe contents. On the other hand, all hydrogels, despite their different swelling capacity, present a total degradation during the first 20–24 days in a hydrolytic medium and 5–10 days in enzymatic medium with lysozyme and hyaluronidase. In addition, apart from biocompatibility, all hydrogels, demonstrated regardless their composition, an excellent and fast ability to self-recover their shape after being damaged.

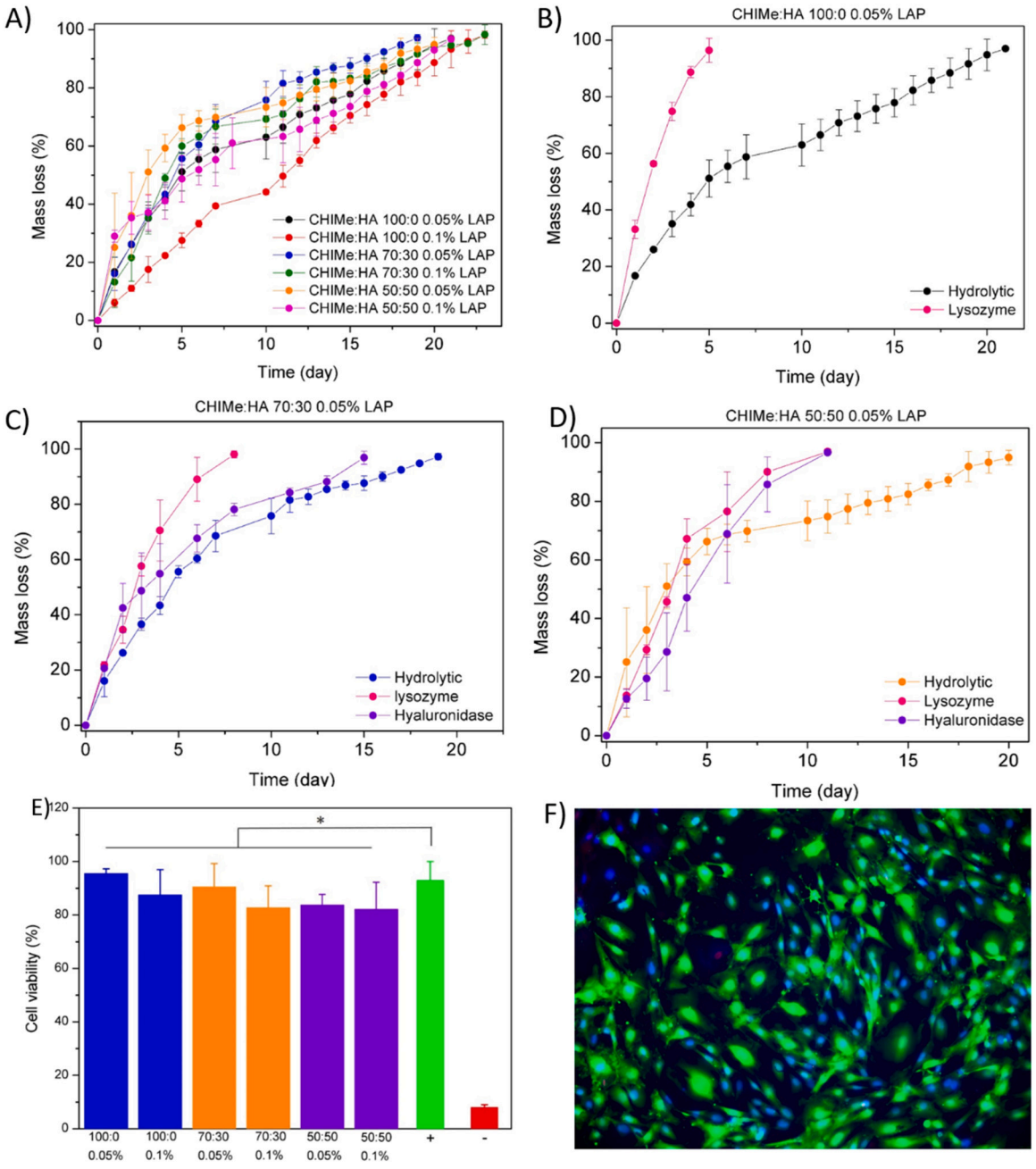

Fig. 8. Degradation profiles in A) hydroltic media of different hydrogels and enzymatic degradation of B) 100 % CHIMe based hydrogel with 0.05 % of LAP C) 70:30 CHIM:HA based hydrogel with 0.05 % of LAP and D) 50:50 CHIMe: HA based hydrogel with 0.05 % of LAP. E) Biocompatibility of the CHIMe:HA hydrogels polymerized in the presence of different amounts of LAP. One-way ANOVA test with Tukey's multiple comparison test was used for the statistical analysis ($p < 0.05$). Cell survival after 24-h incubation with CHIMe:HA gels showed no statistical differences (*) from control wells without hydrogel and F) Fluorescence images of the blue (NucBlue, cell nuclei), green (calcein, cytoplasm of live cells, control) and red (EthD-1, nuclei of dead cells) cultured in CHIMe:HA 100:0 with 0.05 % LAP content.

Declaration of competing interest

All the authors declare that they have no conflicts of interest.

Data availability

Data will be made available on request.

Acknowledgments

The authors acknowledge funding by Spanish State Research Agency (AEI) and the European Regional Development Fund (ERFD) through the project PID2019-106099RB-C43/AEI/10.13039/501100011033, as well as, from the Basque Government Industry Department under the ELKARTEK program (KK-2021/00040). The authors thank Dra. Cristina Eguizabal for giving them access to the laboratory "Cell Therapy, Stem Cells and Tissue" at the Basque Center of Transfusion and Human at the Galdako hospital. Technical and human support provided by SGIker (UPV/EHU, MICINN, GV/EJ, EGEF and ESF) is gratefully acknowledged.

References

[1] M.N. Collins, F. Zamboni, A. Serafin, A. Escobar, R. Stepanian, M. Culebras, J. M. Oliveira, Emerging scaffold- and cellular-based strategies for brain tissue regeneration and imaging, In Vitro Models 1 (2) (2022) 129–150, https://doi.org/10.1007/s44164-022-00013-0.

[2] K.T. Nguyen, J.L. West, Photopolymerizable hydrogels for tissue engineering applications, Biomaterials 23 (1) (2002) 4307–4314.

[3] K.A. Smeds, M.W. Grinstaff, Photocrosslinkable polysaccharides for in situ hydrogel formation, J. Biomed. Mater. Res. 54 (1) (2001) 115–121, https://doi.org/10.1002/1097-4636(200101)54:1<115::AID-JBM14>3.0.CO;2-Q.

[4] J. Pan, J. Deng, L. Yu, Y. Wang, W. Zhang, X. Han, Y. Liu, Investigating the repair of alveolar bone defects by gelatin methacrylate hydrogels-encapsulated human periodontal ligament stem cells, J. Mater. Sci. Mater. Med. 31 (1) (2020), https://doi.org/10.1007/s10856-019-6333-8.

[5] N. Monteiro, G. Thrivikraman, A. Athirasala, A. Tahayeri, C.M. França, J. L. Ferracane, L.E. Bertassoni, Photopolymerization of cell-laden gelatin methacryloyl hydrogels using a dental curing light for regenerative dentistry, Dent. Mater. 34 (3) (2018) 389–399, https://doi.org/10.1016/j.dental.2017.11.020.

[6] J.R. Choi, K.W. Yong, J.Y. Choi, A.C. Cowie, Recent advances in photo-crosslinkable hydrogels for biomedical applications, BioTechniques 66 (2019) 40–53.

[7] J.B. Leach, K.A. Bivens, C.N. Collins, C.E. Schmidt, Development of photocrosslinkable hyaluronic acid-polyethylene glycol-peptide composite hydrogels for soft tissue engineering, J.Biomed.Mater.Res.A 70 (1) (2004) 74–82, https://doi.org/10.1002/jbm.a.30063.

[8] S.H. Kim, C.C. Chu, Synthesis and characterization of dextran-methacrylate hydrogels and structural study by SEM, J. Biomed. Mater. Res. 49 (4) (2000) 517–527, https://doi.org/10.1002/(SICI)1097-4636(20000315)49:4<517::AID-JBM10>3.0.CO;2-8.

[9] G. Bayramoglu, Metacrylated chitosan baed UV curable support for enzyme immobilization, Mater. Res. 20 (2) (2012) 452–459.

[10] M. Sahranavard, A. Zamanian, F. Ghorbani, M.H. Shahrezaee, A critical review on three dimensional-printed chitosan hydrogels for development of tissue engineering, Bioprinting 17 (January 2019) (2020), e00063, https://doi.org/10.1016/j.bprint.2019.e00063.

[11] M. Collado-González, Y.G. Espinosa, F.M. Goycoolea, Interaction between chitosan and mucin: fundamentals and applications, Biomimetics 4 (2) (2019) 1–20, https://doi.org/10.3390/biomimetics4020032.

[12] R. Logithkumar, A. Keshavnarayan, S. Dhivya, A. Chawla, S. Saravanan, N. Selvamurugan, A review of chitosan and its derivatives in bone tissue engineering, Carbohydr. Polym. 151 (2016) 172–188, https://doi.org/10.1016/j.carbpol.2016.05.049.

[13] B.L. Oss-ronen, D. Seliktar, Photopolymerizable hydrogels made from polymer-conjugated albumin for affinity-based drug delivery, Adv.Biomater. 12 (1) (2010) 845–852, https://doi.org/10.1002/adem.200980005.

[14] J.L. West, J.A. Hubbell, Reactive polymers photopolymerized hydrogel materials for drug delivery applications, React. Polym. 25 (1) (1995) 139–147.

[15] J. Hu, Y. Hou, H. Park, B. Choi, S. Hou, A. Chung, M. Lee, Visible light crosslinkable chitosan hydrogels for tissue engineering, Acta Biomater. 8 (5) (2012) 1730–1738.

[16] O.M. Kolawole, W.M. Lau, V.V. Khutoryanskiy, Methacrylated chitosan as a polymer with enhanced mucoadhesive properties for transmucosal drug delivery, Int. J. Pharm. 550 (1–2) (2018) 123–129, https://doi.org/10.1016/j.ijpharm.2018.08.034.

[17] L.M.Y. Yu, K. Kazazian, M.S. Shoichet, Peptide surface modification of methacrylamide chitosan for neural tissue engineering applications, J. Biomed. Mater. Res. A 79 (4) (2008) 963–973, 10.1002/jbm.a.

[18] S. Maiz-Fernández, N. Barroso, L. Pérez-Álvarez, U. Silván, J.L. Vilas-Vilela, S. Lanceros-Mendez, 3D printable self-healing hyaluronic acid/chitosan polycomplex hydrogels with drug release capability, Int. J. Biol. Macromol. 188 (June) (2021) 820–832, https://doi.org/10.1016/j.ijbiomac.2021.08.022.

[19] S. Maiz-Fernández, L. Pérez-álvarez, L. Ruiz-Rubio, J.L. Vilas-Vilela, S. Lanceros-Mendez, Polysaccharide-based in situ self-healing hydrogels for tissue engineering applications, Polymers 12 (10) (2020) 1–33, https://doi.org/10.3390/polym12102261.

[20] Y. Tu, N. Chen, C. Li, H. Liu, R. Zhu, S. Chen, L. He, Advances in injectable self-healing biomedical hydrogels, Acta Biomater. 90 (2019) 1–20, https://doi.org/10.1016/j.actbio.2019.03.057.

[21] N.V. Dubashynskaya, S.V. Raik, Y.A. Dubrovskii, E.V. Demyanova, E. S. Shcherbakova, D.N. Poshina, Y.A. Skorik, Hyaluronan/diethylaminoethyl chitosan polyelectrolyte complexes as carriers for improved colistin delivery, Int. J. Mol. Sci. 22 (16) (2021), https://doi.org/10.3390/ijms22168381.

[22] S.D. Nath, C. Abueva, B. Kim, B.T. Lee, Chitosan-hyaluronic acid polyelectrolyte complex scaffold crosslinked with genipin for immobilization and controlled release of BMP-2, Carbohydr. Polym. 115 (2015) 207–214, https://doi.org/10.1016/j.carbpol.2014.08.077.

[23] C. Tonda-Turo, I. Carmagnola, A. Chiappone, Z. Feng, G. Ciardelli, M. Hakkarainen, M. Sangermano, Photocurable chitosan as bioink for cellularized therapies towards personalized scaffold architecture, Bioprinting 18 (December 2019) (2020), e00082, https://doi.org/10.1016/j.bprint.2020.e00082.

[24] A.R. Osi, H. Zhang, J. Chen, Y. Zhou, R. Wang, J. Fu, Q. Zhong, Three-dimensional-printable thermo/photo-cross-linked methacrylated chitosan-gelatin hydrogel composites for tissue engineering, ACS Appl. Mater. Interfaces 13 (19) (2021) 22902–22913, https://doi.org/10.1021/acsami.1c01321.

[25] D. Lu, Z. Zeng, Z. Geng, C. Guo, D. Pei, J. Zhang, S. Yu, Macroporous methacrylated hyaluronic acid hydrogel with different pore sizes for in vitro and in vivo evaluation of vascularization, Biomed.Mater.(Bristol) 17 (2) (2022), https://doi.org/10.1088/1748-605X/ac494b.

[26] Y.M. Chung, K.L. Simmons, A. Gutowska, B. Jeong, Sol-gel transition temperature of PLGA-g-PEG aqueous solutions, Biomacromolecules 3 (3) (2002) 511–516, https://doi.org/10.1021/bm0156431.

[27] S. Tanodekaew, J. Godward, F. Heatley, C. Booth, Gelation of aqueous solutions of diblock copolymers of ethylene oxide and D,L-latcide, Macromol. Chem. Phys. 198 (11) (1997) 3385–3395.

[28] C. Mendes-Felipe, M. Salado, L.C. Fernandes, D.M. Correia, L. Ruiz-Rubio, M. Tariq, S. Lanceros-Mendez, Photocurable temperature activated humidity hybrid sensing materials for multifunctional coatings, Polymer 221 (March) (2021) 1–11, https://doi.org/10.1016/j.polymer.2021.123635.

[29] J. Schindelin, I. Arganda-Carreras, E.F. Verena Kaynig, M. Longair, T. Pietzsch, S. Preibisch, A. Cardona, Fiji: an open-source platform for biological-image analysis, Nat. Methods 9 (7) (2012) 676–682, https://doi.org/10.1038/nmeth.2019.

[30] P. Erkoc, Y.N. Odeh, N. Alrifai, O. Zirhli, N. Gunduz Akdogan, B. Yildiz, O. Akdogan, Photocurable pentaerythritol triacrylate/lithium phenyl-2,4,6-trimethylbenzoylphosphinate-based ink for extrusion-based 3D printing of magneto-responsive materials, J. Appl. Polym. Sci. 137 (35) (2020) 1–10, https://doi.org/10.1002/app.49043.

[31] N. Barroso, O. Guaresti, L. Pérez-Álvarez, L. Ruiz-Rubio, N. Gabilondo, J.L. Vilas-Vilela, Self-healable hyaluronic acid/chitosan polyelectrolyte complex hydrogels and multilayers, Eur. Polym. J. 120 (July) (2019), 109268, https://doi.org/10.1016/j.eurpolymj.2019.109268.

[32] L. Ruiz-Rubio, E. Lizundia, J.L. Vilas, L.M. León, M. Rodríguez, Influence of N-alkyl and α-substitutions on the thermal behaviour of H-bonded interpolymer complexes based on polymers with acrylamide or lactame groups and poly(4-vinylphenol), Thermochim. Acta 614 (2015) 191–198, https://doi.org/10.1016/j.tca.2015.06.030.

[33] R. Servaty, J. Schiller, H. Binder, K. Arnold, Hydration of polymeric components of cartilage - an infrared spectroscopic study on hyaluronic acid and chondroitin sulfate, Int. J. Biol. Macromol. 28 (2) (2001) 121–127, https://doi.org/10.1016/S0141-8130(00)00161-6.

[34] K. Van De Velde, P. Kiekens, Structure analysis and degree of substitution of chitin, chitosan and dibutyrylchitin by FT-IR spectroscopy and solid state13C NMR, Carbohydr. Polym. 58 (4) (2004) 409–416, https://doi.org/10.1016/j.carbpol.2004.08.004.

[35] X. Xu, A.K. Jha, D.A. Harrington, M.C. Farach-Carson, X. Jia, Hyaluronic acid-based hydrogels: from a natural polysaccharide to complex networks, Soft Matter 8 (12) (2012) 3280–3294, https://doi.org/10.1039/C2SM06463D.

[36] S. Maiz-Fernández, O. Guaresti, L. Pérez-Álvarez, L. Ruiz-Rubio, N. Gabilondo, J. L. Vilas-Vilela, S. Lanceros-Mendez, β-Glycerol phosphate/genipin chitosan hydrogels: a comparative study of their properties and diclofenac delivery, Carbohydr. Polym. 248 (July) (2020), 116811, https://doi.org/10.1016/j.carbpol.2020.116811.

[37] T. Kean, M. Thanou, Biodegradation, biodistribution and toxicity of chitosan, Adv. Drug Deliv. Rev. 62 (1) (2010) 3–11, https://doi.org/10.1016/j.addr.2009.09.004.

[38] A. Loncarevic, M. Invankovic, A. Rogina, Lysozyme-induced degradation of chitosan: the characterisation of degraded chitosan scaffolds, J.Tissue Repair Regen. 1 (1) (2017) 23–27, https://doi.org/10.14302/issn.2640.

[39] M.K. Paap, R.Z. Silkiss, The interaction between hyaluronidase and hyaluronic acid gel fillers - a review of the literature and comparative analysis, Plast.Aesthet.Res. 2020 (2020), https://doi.org/10.20517/2347-9264.2020.121.

[40] K. Fan, D. Gonzales, M. Sevoian, Hydrolytic and enzymatic degradation of poly(y-glutamic acid) hydrogels and their application in slow-release systems for proteins, J.Environ.Polym.Degrad. 4 (4) (1996) 253–260, https://doi.org/10.1007/bf02070694.